

RSC Advances



This is an *Accepted Manuscript*, which has been through the Royal Society of Chemistry peer review process and has been accepted for publication.

Accepted Manuscripts are published online shortly after acceptance, before technical editing, formatting and proof reading. Using this free service, authors can make their results available to the community, in citable form, before we publish the edited article. This *Accepted Manuscript* will be replaced by the edited, formatted and paginated article as soon as this is available.

You can find more information about *Accepted Manuscripts* in the [Information for Authors](#).

Please note that technical editing may introduce minor changes to the text and/or graphics, which may alter content. The journal's standard [Terms & Conditions](#) and the [Ethical guidelines](#) still apply. In no event shall the Royal Society of Chemistry be held responsible for any errors or omissions in this *Accepted Manuscript* or any consequences arising from the use of any information it contains.

27 **Abstract**

28 Coking wastewater discharge can lead to pollution, due to water reuse or release to
29 surface water after the disinfection process. In this work, the dissolved organic matter
30 (DOM) in effluent was isolated into 42 classes using molecular weight distribution
31 and resin adsorbents. The trihalomethane and haloacetonitrile formation potential
32 (THMFP and HANFP) from each fraction were measured and correlated with the
33 UV-Vis absorption and fluorescence excitation-emission matrix (EEM), and the
34 compounds in the classes as precursors were determined by solid phase extraction,
35 silica chromatography and GC/MS. The results show that the highest SUVA in
36 the >100 kDa fraction was $12.1 \text{ L} \cdot \text{mg}^{-1} \cdot \text{cm}^{-1}$. The lower MW fractions (5-10 kDa, 3-5
37 kDa, 1-3 kDa and <1 kDa) had similar SUVA about $4.1 \text{ L} \cdot \text{mg}^{-1} \cdot \text{cm}^{-1}$. The HiA
38 (Hydrophilic acids) fraction was found to be the most abundant, constituting about 45%
39 of DOC. The THMFP and HANFP show that the DOM fraction with low MW and
40 HiA was the dominant fraction and contributed more precursors. The EEM spectra
41 indicated there were notable amounts of soluble microbial products and aromatic
42 proteins in the >100 kDa fraction. Based on the results of the GC/MS analysis, nitriles,
43 amines, nitrogenous heterocyclics, hydrocarbons, polycyclic aromatic hydrocarbons,
44 esters, phenols, alcohol, ketones, and organic acids determined as precursors in the <1
45 kDa fraction. Both precursors have functional groups with high chlorine reactivity,
46 such as carboxylate salt COO^- , aromatic structures $\text{C}=\text{C}$, aldehydes and ketones
47 groups $\text{C}=\text{O}$, carbohydrates $\text{C}-\text{C}$ and O-alkyl group $\text{C}-\text{O}$ contributing greatly to the
48 formation of disinfection by-production precursors.

49 **Key words:** coking wastewater; chlorination; disinfection by-production precursors;
50 fraction; organic functional groups.

51

52 **1. Introduction**

53 The steel industry generates various wastewaters during the manufacturing and
54 processing of iron, and this known as coking wastewater, which is very toxic and thus
55 needs to be treated before being discharged into the environment. This wastewater is
56 mostly generated from cooling step after heating the coking coals to a high

57 temperature (900-1100 °C) and the liquid-stripping step of the produced coke oven
58 gas^[1-3], and contains various toxic compounds such as ammonia, thiocyanide,
59 cyanides, phenols, nitrogenous heterocyclic compounds and polycyclic aromatic
60 hydrocarbons in a high concentration range^[4]. China has the largest coke production
61 and exports in the world, with more than 40% of global coke output and more than 60%
62 of global coke exports. This leads to the production of more than 200 million tons
63 coking wastewater each year^[5]. The Chinese government issued the consultation of
64 Technical Specifications for Coking Wastewater Treatment in 2010, which proposed
65 that the treated coking wastewater should be preferred direct reused or recycled after
66 thorough purification, with the aim of gradually achieving zero discharge of coking
67 wastewater after treatment^[6]. Wastewater reuse is increasingly regarded as a potential
68 water resource way to reduce pressure on existing water supplies. Most sewage
69 treatment plants receive complex mixtures of urban and industrialized discharges.
70 Even after secondary treatment, they still contain a large amount of dissolved organic
71 matter (DOM), which serves as a precursor in the chlorination process and can lead to
72 the formation of potentially harmful disinfection by-products (DBPs) including
73 trihalomethanes (THMs), haloacetonitriles (HANs)^[7-9]. The chemical characteristics
74 of DOM are thought to significantly influence the chlorine consumption and
75 formation of DBPs. Therefore, the effects of the characteristics of DOM in the
76 discharge of coking wastewater treatment plant with regard to the formation of DBPs
77 are an issue that requires more research.

78 Compared with natural water, the compositions of DOM in biologically treated
79 coking wastewater are more complex and distinct, containing a heterogeneous
80 mixture of synthetic organic chemicals produced during coking production, as well as
81 soluble microbial products. The reactions that occur between chlorine and DOM
82 during wastewater chlorination are significantly more complex than those that occur
83 during chlorine disinfection of drinking water^[10, 11]. As a result, fractionation of DOM
84 is required to better understand the formation of DBPs in biologically treated
85 wastewater during the chlorine disinfection process. Resin isolation is the currently
86 most common method for the fractionation of DOM in biologically treated

87 wastewater^[12]. Different resins can fractionate DOM into various components (e.g.
88 hydrophobic and hydrophilic fractions) that meet specific research needs based on the
89 chemical properties of DOM. About 90% of the DOM in the water tested in most
90 studies was recovered by using the resin adsorption method^[13]. An ultra-filtration (UF)
91 membrane is commonly used to fraction and measure DOM by molecular weight
92 distribution, with UF separation being more efficient than resin adsorption with regard
93 to this^[14]. The strong acidic and basic treatment required in the resin adsorption
94 process may change the characteristics of DOM and result in hydrolysis and other
95 reactions^[15]. Therefore, combining with resin adsorption and UF separation in the
96 fractionation of DOM is a better method of realizing the characteristics of DOM. The
97 relationship between the formation of THMs or HANs and chlorine kinetics with
98 regard to DOM molecular size during the chlorine disinfection of natural water or
99 municipal wastewater has been widely investigated in previous research^[16-18].
100 However, few studies examine the role of DOM molecular size in the formation DBPs
101 during the chlorination of biologically treated industrial wastewater.

102 The characteristics of DOM, such as the amount of dissolved organic carbon
103 (DOC), ultraviolet absorbance at 254 nm (UV₂₅₄), specific UV absorbance (SUVA),
104 excitation emission matrix (EEM), fluorescence regional integration (FRI), molecular
105 weight and hydrophobicity have been studied in water and wastewater from different
106 sources^[19-22]. In order to determine the chlorination of DBP precursors in each
107 fraction, it is better to apply the method of gas chromatography-mass spectrometry
108 (GC-MS) after separating them. However, the chemical compounds in coking
109 wastewater discharge are very small, complicated and numerous. Solid phase
110 extraction is a simple and convenient sample pre-treatment technology, which
111 integrates the extraction and enrichment of organic from wastewater. It has been
112 applied in micro-organic pollution detection in relation to PCBs and PAHs in different
113 environmental media^[3, 6]. Silica column chromatography can collect different
114 polarities of organic compounds according to the different eluents, and is suitable for
115 use with complex coking wastewater discharge. It is therefore necessary to establish a
116 solid phase extraction, silica column chromatography and GC-MS analysis method to

117 determine the DBPs precursors in coking wastewater, in order to obtain detail of the
118 chemical composition and the general concentration levels in it.

119 The main objective of the present study was thus to investigate the
120 characteristics of DOM in coking wastewater discharge, the associations of these with
121 the formation of THMs and HANs, and the identification of DBPs precursors.
122 Fractionation of the coking wastewater discharge was conducted by using UF
123 separation and resin adsorption in turn. Dissolved organic matter (DOC), UV_{254} and
124 EEM were then used to quantify NOM in each part of the fractionated samples. After
125 chlorination, THMs and HANs were analyzed in the solutions, and the links between
126 DBPs and NOM were further examined. Moreover, the organic components with the
127 highest disinfection by-product formation potential were detected by GC-MS. The
128 results can provide important information with regard to the new DBPs precursors and
129 their reactivity in relation to the formation of DBPs.

130 2. Material and methods

131 2.1 Wastewater samples

132 Wastewater samples were collected from a coking wastewater treatment plant at
133 Songshan coking plant in Shangan, Guangdong Province of China, with an average
134 treatment capacity of $2000 \text{ m}^3 \cdot \text{d}^{-1}$. The plant has primary treatment process that
135 includes a flotation-degreasing tank and an equalization basin, an anoxic-oxic-oxic
136 system coupled with a biological fluidized bed, a biological aerated filter and
137 coagulation. The coking wastewater consists of distilled ammonia wastewater,
138 desulfurization waste solution and domestic wastewater. The monthly average
139 characteristics of the coking wastewater discharge are listed in Table.1.

140 Table.1 Main physical and chemical properties of coking wastewater discharge in this
141 plant

Parameter	Concentration (mean)	Unit
Temperature	24 ± 2	$^{\circ}\text{C}$
pH	7.4 ± 0.3	
COD_{Cr}	84.6 ± 5.4	$\text{mg} \cdot \text{L}^{-1}$

TOC	32.1 ± 2.6	mg·L ⁻¹
BOD ₅	7.65 ± 0.81	mg·L ⁻¹
NH ₄ -N	4.51 ± 1.25	mg·L ⁻¹
CN ⁻	0.046 ± 0.005	mg·L ⁻¹
NO ₃ ⁻	151.2 ± 5.6	mg·L ⁻¹
SO ₄ ²⁻	0.84 ± 0.08	mg·L ⁻¹
PO ₄ ³⁻	0.32 ± 0.04	mg·L ⁻¹
S ²⁻	0.14 ± 0.02	mg·L ⁻¹
F ⁻	41.6 ± 1.8	mg·L ⁻¹
Cl ⁻	681.2 ± 5.9	mg·L ⁻¹
Br ⁻	15.05 ± 1.6	mg·L ⁻¹
I ⁻	5.12 ± 0.7	mg·L ⁻¹
Ca ²⁺	90.82 ± 3.64	mg·L ⁻¹
Mg ²⁺	7.59 ± 1.52	mg·L ⁻¹
Na ⁺	1135.2 ± 8.69	mg·L ⁻¹
Conductivity	3.35 ± 0.68	Ms·cm ⁻¹
Turbidity	32.5 ± 2.65	NTU
Chroma	40 ± 5	
Redox potential(mv)	-23 ± 1	Mv
Suspended solids	1.845 ± 0.36	mg·L ⁻¹

142 2.2 Molecular weight fractionation

143 The raw water was filtered through a 0.45µm cellulose membrane (Sinopharm) in
 144 order to obtain the dissolved organic matter (DOM). The DOM was fractionated using
 145 six types of regenerated cellulose membranes (Millipore Corp): (1)100,000 nominal
 146 molecular weight limit (NWML), (2) 30,000 NWML, (3) 10,000 NWML, (4) 5,000
 147 NWML (5) 3000 NWML, and (6) 1000 NWML. The effective surface area of the
 148 membrane was 31.75 cm². Prior to filtration, Milli-Q water was passed through the
 149 membranes to remove any possible leached organics until the amount of DOC in the
 150 permeate was less than 0.1 mg/L. High purity nitrogen (99.999%) was used to

151 pressurize the filtration process (~0.15 MPa). The initial sample volume was 500 mL.
 152 After 400 mL of sample volume permeated the membrane, the remaining 100 mL was
 153 collected for analysis. The percentages of DOC in each size range were calculated as
 154 follows:

$$155 \quad \% < 1kDa = \frac{C_{1k,permate}}{C_{raw}} \times 100 \quad (1)$$

$$156 \quad \%1k - 3kDa = \frac{C_{3k,permate} - C_{1k,permate}}{C_{raw}} \times 100 \quad (2)$$

$$157 \quad \%3k - 5kDa = \frac{C_{5k,permate} - C_{3k,permate}}{C_{raw}} \times 100 \quad (3)$$

$$158 \quad \%5k - 10kDa = \frac{C_{10k,permate} - C_{5k,permate}}{C_{raw}} \times 100 \quad (4)$$

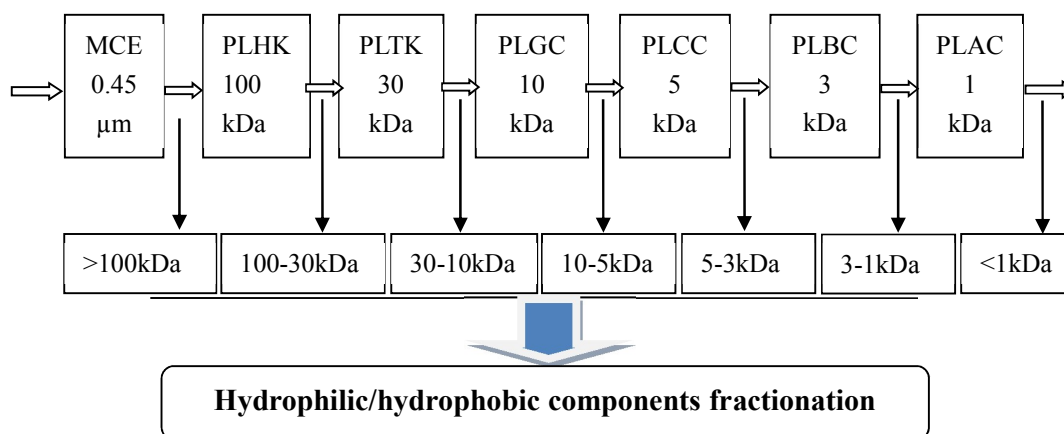
$$159 \quad \%10k - 30kDa = \frac{C_{30k,permate} - C_{10k,permate}}{C_{raw}} \times 100 \quad (5)$$

$$160 \quad \%30k - 100kDa = \frac{C_{100k,permate} - C_{30k,permate}}{C_{raw}} \times 100 \quad (6)$$

$$161 \quad \% > 100kDa = \frac{C_{raw} - C_{100k,permate}}{C_{raw}} \times 100 \quad (7)$$

162 C_{raw} : the concentration of DOC in the raw water

163 C_{nkDa} : the concentration of DOC in each size range



164

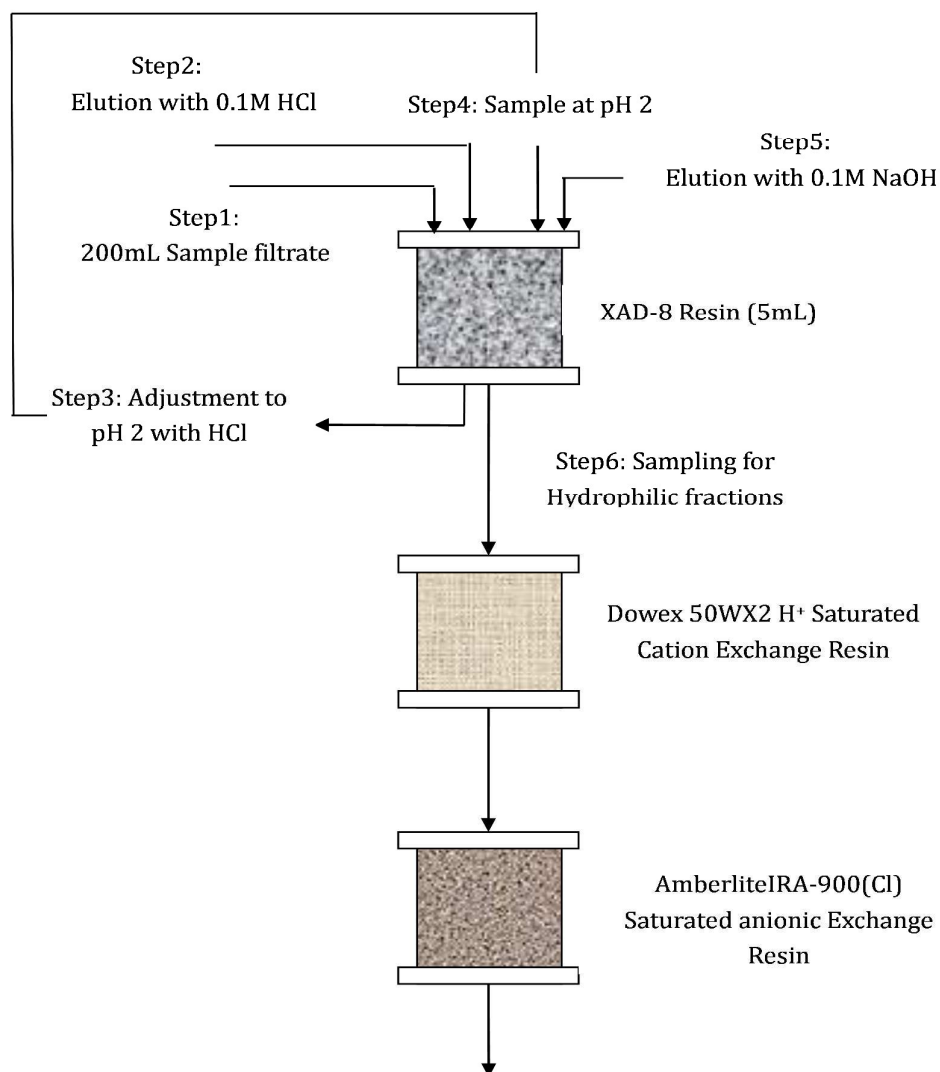
165

Fig. 1. A schematic program for determination of molecular weight cut-off

166 (MCE: Mixed Cellulose Esters; PLHK: Ultracel Millipore 100kDa; PLTK: Ultracel
167 Millipore 30kDa; PLGC: Ultracel Millipore 10kDa; PLCC: Ultracel Millipore 5kDa;
168 PLBC: Ultracel Millipore 3kDa; PLAC Ultracel Millipore 1kDa)

169 **2.3 Hydrophilic/hydrophobic components fractionation**

170 After UF separation of DOM, the adsorbent resin method was followed to use in
171 DOM fractionation. In this, adsorbent resins (Amberlite XAD-8 nonionic resin ,
172 Dowex 50WX2 H⁺ cation exchange resin and Amberlite IRA-900(Cl⁻) anion exchange
173 resin) were used to separate the water-soluble organic substances into six groups:
174 Hydrophobic acids (HoA), Hydrophobic neutrals (HoN), Hydrophobic bases (HoB),
175 Hydrophilic acids (HiA), Hydrophilic neutrals (HiN), and Hydrophilic bases (HiB).
176 The XAD-8 resin, Dowex 50WX2 H⁺ cation exchange resin and Amberlite
177 IRA-900(Cl⁻) anion exchange resin were Soxhlet-extracted with methanol for 24h.
178 The Amberlite IRA-900(Cl⁻) anion exchange resin was then converted into a
179 free-base-form with 1M NaOH and rinsed with Milli-Q water until the pH of the resin
180 slurry was approximately neutral. Five milliliters (wet volume) of the XAD-8 resin
181 was packed into a glass column and rinsed three times, alternating 0.1 M NaOH with
182 0.1M HCl each time, and then rinsed with about 200mL of Milli-Q water just before
183 sample application. Glass columns containing 5 mL (wet volume) of the cation and
184 anion resins were connected in series and conditioned by pumping Milli-Q water
185 through the resins. Blank samples were taken from each column after conditioning. A
186 flow chart of the DOM fractionation procedure is shown in Fig. 2, and this included
187 the following steps. (1) passing 200 mL of the filtrate through the XAD-8 column at a
188 flow rate of about 1mL·min⁻¹, and rinsing the column with two bed volumes of 0.1 M
189 HCl (HoB); (2) acidifying the filtrate to pH 2.0 , pumping it from the XAD-8 column
190 through the series of cation and anion resin columns at a flow rate of about 1
191 mL· min⁻¹, and eluting the column with more than three bed volumes of 0.1 M NaOH
192 at a flow rate not exceeding 0.5 mL·min⁻¹(HoA, HiB and HiA in sequence); (3) the
193 effluent from the series resins columns was HiN, while HoN was adsorbed in XAD-8.



194

195 Fig.2. A flow chart of the DOM fractionation procedure by resin adsorption

196 **2.4 Reagent and analytical methods**

197 THMs and HANs were chosen as typical C-DBP and N-DBP for coking
 198 wastewater discharge disinfection respectively. Most information about DBP yields
 199 from specific precursors comes from laboratory-based formation potential (FP) tests
 200 using activated compounds, such as example $\text{NaClO}^{[23]}$. These tests are designed to
 201 maximize DBP formation and so use an excess of disinfectant, and they typically
 202 consider a contact times of seven days, temperatures of 25 °C and pH 7.0. DBPFP
 203 tests will overestimate DBPs relative to the same precursors exposed to lower
 204 disinfectant concentrations, disinfectant contact times, and temperatures^[24]. DBPFP

205 can thus reveal almost the whole activity of each fractioned sample.

206 The THMs and HANs in Table 2 were generated during pre-chlorination and
 207 disinfection by the reaction between chlorine and some DOM. The concentration of
 208 these organic precursors could be determined as THMFP and HANFP. THMs and
 209 HANs were analyzed in accordance with EPA method 551(USEPA Methods 551.1)^[25].
 210 NaClO (analytical reagent) was used as the disinfection agent in the THMFP and
 211 HANFP measured process. All samples were buffered to pH 7.2 with a phosphate
 212 buffer before chlorination at $m(\text{Cl}_2):m(\text{DOC})=10(\text{DOC calculation with C})$. All
 213 chlorinated samples were stored headspace-free in the dark, at room temperature (25
 214 ± 1 °C) and underwent seven days reaction time. A series of aqueous DBPs standards
 215 was generated by adding a range of volumes of the stock solutions to Milli-Q water. A
 216 blank (0 g/L as DBPs standards) of Milli-Q water was included in the development of
 217 all standard curves. Under the assumption of linear response behavior, the regression
 218 analyses always yielded $R^2>0.99$.

219 Table 2. The species of tested THMs and HANs

DBPs	Formula	Name	Analytical method
	CHCl_3	Chloroform(TCM)	
Trihalomethanes (THMs)	CHCl_2Br	Bromodichloromethane(BDCM)	
	CHBr_2Cl	Dibromochloromethane(DBCM)	
	CHBr_3	Bromoform(TBM)	
Haloacetonitriles (HANs)	$\text{CCl}_3\text{C}\equiv\text{N}$	Trichloroacetonitrile(TCAN)	USEPA Methods 551.1
	$\text{CCl}_2\text{C}\equiv\text{N}$	Dichloroacetonitrile(DCAN)	
	$\text{CHBrClC}\equiv\text{N}$	Bromochloroacetonitrile(BCAN)	
	$\text{CBr}_2\text{C}\equiv\text{N}$	Dibromoacetonitrile(DBAN)	

220 GC-MS analysis: Based on the contents and concentrations of the organic compounds,
 221 1000 mL of fractionation was extracted onto C18 cartridges (Spherigel) .The aqueous
 222 extract was loaded onto a 1:2 alumina/silica gel glass column with 1 g of anhydrous

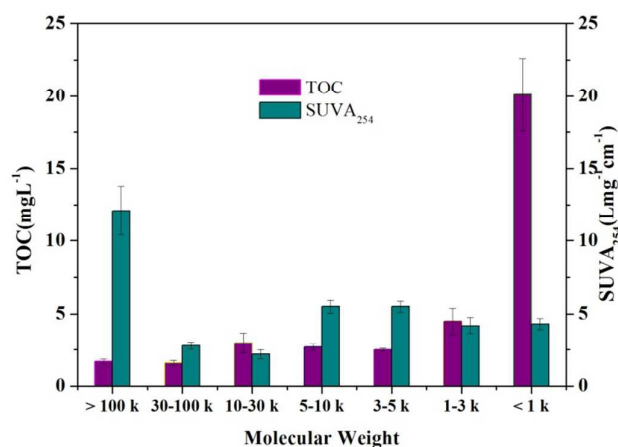
223 sodium sulfate overlaying the silica gel for clean-up and fractionation. First, 15 mL of
224 hexane was applied to remove aliphatic hydrocarbons. The eluents containing
225 medium polarity compounds were then collected by eluting 70 mL of
226 dichloromethane/hexane (3:7, v/v). Finally, the polar compounds were eluted with 30
227 mL methanol and all eluents were concentrated to 0.5 mL under a gentle stream of
228 purified N₂. The samples were analyzed by GC/MS (Agilent, 7890A-5973C) with a
229 30m × 0.25 mm i.d. × 0.25 μm film thickness HP-5 MS fused silica capillary column
230 in selected ion mode. Before sample injection, the polar compounds underwent a
231 derivatization by N,O-Bis (trimethylsilyl) trifluoroacetamide (BSTFA). The steps
232 used in the derivatization are introduced briefly as follows. First, 2.0 mL of an extract
233 was transferred to a 10 mL glass tube (KiMAX, USA) with a polytetrafluoroethylene
234 screw cap. 2.0 mL saturated NaCl aqueous solution was added to the tube, and the
235 solution pH was regulated to < 2. 4.0 mL of dichloromethane was added to the tube,
236 and the tube was tightly capped and manually shaken vigorously for 5 mins, then left
237 at the room temperature for 10 mins. The dichloromethane phase was then carefully
238 transferred to a 10.0 mL glass centrifugal tube using a glass pipette. Another 4.0 mL
239 of dichloromethane was added to the 10.0 mL tube, which was manually shaken for 5
240 mins. After separation, the dichloromethane was transferred to the 10.0 mL glass
241 centrifugal tube and combined with the previous sample. The dichloromethane was
242 then dried under a gentle nitrogen stream. The final extract was re-dissolved in 200
243 μL of acetone, which was transferred to a 2.0 mL amber glass vial. Then 50 μL of 10%
244 pyridine in toluene and 50 μL of 2% BSTFA were added into the amber glass vial in
245 sequence, and the vial was left at room temperature for 1 h. Finally, the samples were
246 ready for GC-MS analysis. The GC/MS conditions for sample analysis were as follow:
247 The injection port, interface line and ion source temperature were maintained at 280,
248 290 and 250 °C, respectively. The column temperature was programmed from 60 to
249 310 °C at 5 °C /min and held for 10 min. Helium was the carrier gas at a flow of 1.2
250 mL/min with a linear velocity of 42.4 cm/s. The mass spectrometer was operated in
251 electron impact ionization mode (70eV). 1 μL volume of each sample was injected in
252 the split mode; the split ratio was 10:1.

253 DOC measurements were conducted as non-purgeable DOC with a Shimadzu
254 TOC-VCPH. At least three measurements were made for each sample. Ultraviolet
255 (UV) absorbance was measured with a Shimadzu UV-2500 UV/VIS spectrometer at
256 254 nm using a quartz cell with a 1-cm path length. Three-dimensional EEM
257 spectroscopy (HITACHI F-7000 FL, 5J1-004, Japan) was also applied to characterize
258 the organic compounds. The pH value was measured with a pH meter (pHS-3C,
259 China).

260 EEM fluorescence spectra were recorded using a Hitachi F-7000 fluorescence
261 spectrometer (Hitachi High-Technologies, Tokyo, Japan). Excitation (Ex) and
262 emission (Em) slit widths were set to 5 nm and PMT Voltage to 400 V with scanning
263 speed at 1200 nm · min⁻¹. The Em was determined every 5 nm from 280 to 550 nm,
264 while the Ex region was set every 2 nm from 200 to 450 nm. Before analysis, the
265 Raman scattering and Rayleigh scatter effects should be removed^[26].

266 3. Results and discussion

267 3.1 SUVA and TOC of different molecular fraction of the coking wastewater 268 discharge

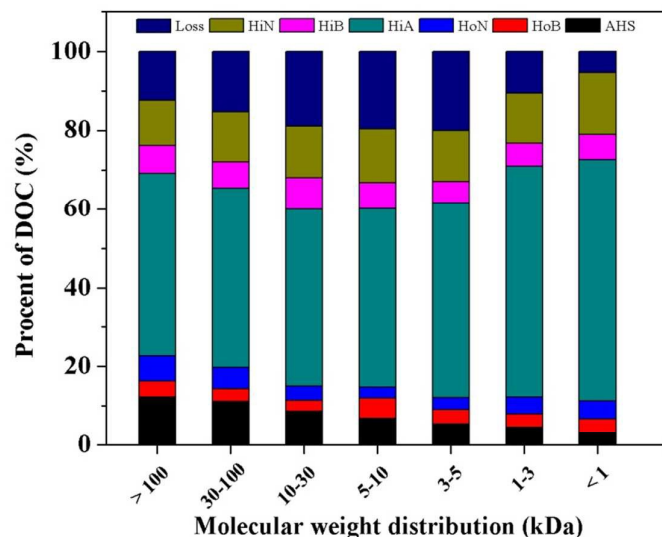


269
270 Fig.3 TOC and SUVA₂₅₄ of different molecular weight fractions of treated coking
271 wastewater discharge

272 Although the quality of coking wastewater discharge can meet the national
273 discharge standards (GB 12356-2012)^[27], some organic components still exist in it,
274 including phenols, amines, and nitrogen heterocyclic, which have high levels of
275 activity in the disinfection process. In our best knowledge, DOM act as a group of

276 DBP precursors, and SUVA is defined as UV_{254} by DOC, which can be a useful
277 indicator for the characteristics of DOM. A low SUVA value implies the water
278 contains few aromatic carbons and is more hydrophilic [28,29]. The raw water samples
279 from the coking wastewater treatment plant were filtered through a series of UF
280 membranes to characterize the DOM species in each size fraction. TOC and UV_{254}
281 were also measured at the same time. Figure 3 shows the TOC and SUVA
282 compositions in each of the MW fractions. Based on the TOC data, the MW fractions
283 of >100k, 30-100k, 10-30k, 5-10k, 3-5k, 1-3k and <1kDa were 1.7, 1.6, 3.0, 2.7, 2.5,
284 4.5 and 20.1 $mg \cdot L^{-1}$, respectively. Given that the MW fractions of <1kDa accounted
285 for approximately 55.7% of the total TOC concentrations, it was concluded that the
286 most of the TOC present in coking wastewater discharge was composed of small
287 molecules. Moreover, the percentage of SUVA was slightly lower in the <1kDa
288 fraction of the sample than other fractions. The highest SUVA was found in
289 the >100kDa fraction at $12.1 L \cdot mg^{-1} \cdot cm^{-1}$. The lower MW fractions (5-10k, 3-5k,
290 1-3k and <1kDa) had similar SUVA about $4.1 L \cdot mg^{-1} \cdot cm^{-1}$. The DOM in coking
291 wastewater had different components, even though the total DOC concentration in
292 each of the water samples was approximately the same. It can thus be concluded that
293 some hydrophobic, aromatic and unsaturated organic matter existed in the >100kDa
294 fraction, like extracellular polymers and microorganism metabolites. The high TOC of
295 the <1kDa fraction showed that a variety of organic compounds still remained in the
296 coking wastewater. Both the >100kDa and the <1kDa fractions could have high levels
297 of activity with regard to DBP generation.

298 **3.2 Hydrophilic and hydrophobic fractions of DOM**



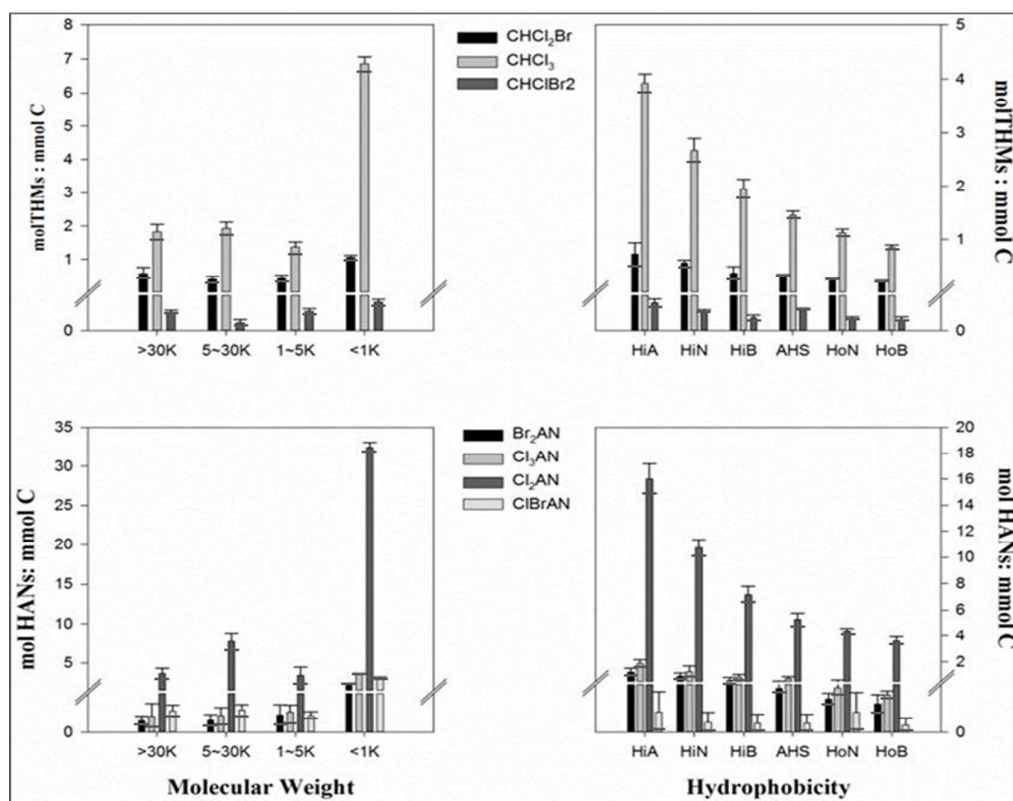
299

300 Fig.4. The distribution of hydrophilic and hydrophobic fractions in the DOC of coking
301 wastewater discharge.

302 Using UF membrane and resin separation fractionation, 42 fractions were chosen
303 to show the characteristics of DOM. Figure 4 presents the results of distribution of
304 hydrophilic and hydrophobic fractions in the DOC of the coking wastewater discharge.
305 The fraction of hydrophilic DOM was higher than that of hydrophobic DOM in
306 different molecular weight distributions. In particular, the HiA fraction was found to
307 be the most abundant fraction, constituting about 45% of DOC. HiN was the second
308 most dominant fraction, accounting for about 15%. The amount of HoB and HoN
309 were similar, at about 4%, the lowest of all the fractions. The amount of AHS fell
310 gradually along with the molecular weight. The DOM-fraction distribution varies
311 significantly depending on the kind of wastewater and type of treatment process. In
312 this study it was found that the percentage of hydrophilic organic compounds was
313 higher than that of the hydrophobic organic compounds, and the acid part was the
314 most common among the fractions. This may be because a large amount of
315 hydrophobic organic matter was degraded by microorganisms or adsorbed during the
316 activated sludge process^[22]. On the other hand, microbial aerobic respiration could
317 produce some carboxylic acid and alcohol, leading to a more acid in the coking
318 wastewater discharge^[30].

319 **3.3 THMs and HANs formation potentials (THMFP and HANFP) of DOM**

320 fractions



321

322 Fig. 5. Distribution of DBPFP with weight and hydrophobicity (a) THMs, (b) HANs.

323 (Cl₂ dose=10:1, temperature=25 °C, Reaction time=7d)

324 In order to investigate the reactivity with chlorine on a per carbon basis, all the
 325 DBPs data were normalized relative to the DOM concentrations to obtain the specific
 326 yields. In this study, DBP yields were determined for two types of halogenated DBPs,
 327 namely, THMs and HANs, using chlorination. Figure 5 shows the THMFPP and
 328 HANFP in each fraction by different molecular weights and degrees of
 329 hydrophobicity of coking wastewater discharge. There were only three THM species
 330 formed in each fraction during the chlorination experiments, namely, chloroform,
 331 biomodichloromethane, and dibromochloromethane. The concentration of biomofom
 332 was below the detection limit, which is consistent with the results of earlier research.
 333 The MW fraction of <1kDa contained the maximum concentration of THMFPP (7.01
 334 mol THM:mmol C, i.e., 53.9% of the total THMFPP), and the >30, 5-30, 1-5 and
 335 <1kDa, fractions contained steadily decreasing concentrations of THMFPP. The results
 336 indicates that DOM with <1kDa is a dominant factor in the formation of THMs during

337 the chlorination process. According to the levels of hydrophobicity, the HiA fraction
338 contained the maximum concentration of THMFP (4.31 mol THM:mmol C, i.e., 89.9%
339 of the total THMFP), and the HiN, HiB, AHS, HoN and HoB, fractions contained
340 decreasing concentrations of THMFP. The results indicate that HiA is also a dominant
341 factor in the formation of THMs, which was also found in the work of Chang^[31].
342 Generally, high MW fractions contain more aliphatic groups in surface water, whereas
343 low MW fractions contain more aromatic and carboxyl groups, which are more
344 reactive to the formation of THMs during chlorination. The small size DOM in treated
345 coking wastewater was more reactive to form THMs in the disinfection process. It
346 was found that HiN contained relatively more humic acid and thus had greater
347 chlorine reactivity.

348 In the HANFP experiments, four HAN species were detected, i.e.,
349 trichloroacetonitrile, dichloroacetonitrile, bromochloroacetonitrile and
350 dibromoacetonitrile. Similar to the distribution of THMFP, the <1kDa MW fraction
351 contained most of the HANFP, followed by the >30, 5-30, 1-5 and <1kDa fractions in
352 decreasing order. The HiA fraction is more reactive with regard to the formation of
353 dichloroacetonitrile than other HANs, which have the same level of reactivity as each
354 other. It has been reported that HANs are produced from the chlorination of selected
355 free amino acids, heterocyclic nitrogen in nucleic acids, proteinaceous materials, and
356 combined amino acids bound to humic structures^[17]. A low MW and hydrophilic
357 fraction, like nitrile or aldehyde, can act as HANs' precursors.

358 In terms of controlling DBPs in the chlorination process, the results of DBPFP in
359 each fraction in this study pose a challenge to plant designers, because most of the
360 currently employed physical and chemical treatment processes are not capable of
361 removing low MW and hydrophilic organics effectively.

362 **3.4 Analysis of Br-DBPFP for different fractions of treated coking wastewater**

363

364

365

366

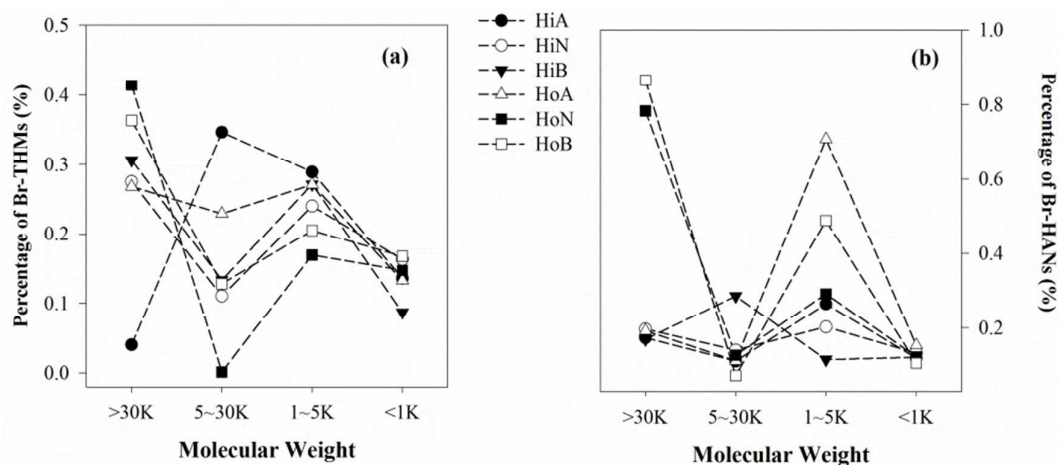
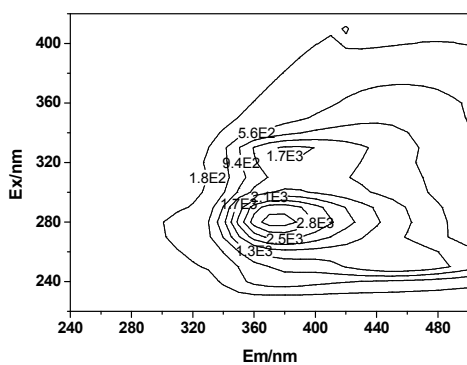
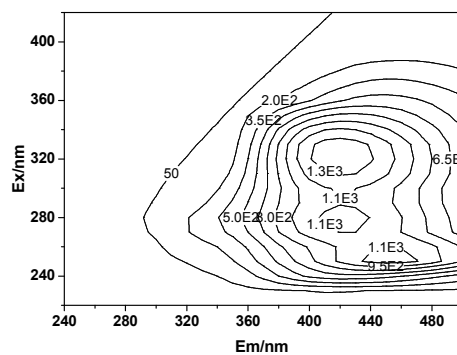


Fig. 6 Percentages of Br-DBPFP for different fractions of treated coking wastewater (Cl_2 dose=10:1, temperature= 25°C , reaction time=7d)

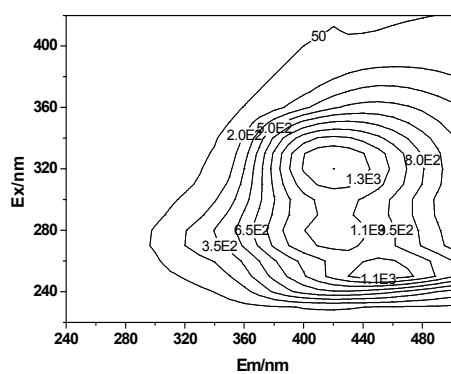
Bromide ions are nearly ubiquitous in coking wastewater discharge, and chlorine can rapidly oxidize bromide ions in the waters to form bromine during the chlorination process. Bromine and chlorine are active oxidants that react with organic matter to produce halogenated DBPs. Bromine is a more efficient substituting agent than chlorine, as it participates in more oxidation reactions. Bromide concentrations thus have a significant impact on the formation and speciation of DBPs. The formation of DBPs shifts to more brominated species as the bromide concentration increase^[32]. The percentages of Br-DBPFP for each fraction of coking wastewater discharge are shown in Figure 6. With regard to the molecular weight distribution, bromine DBPs are readily generated with a low molecular weight of organic matter. Acidic organic matters are more reactive than alkaline compounds with regard to bromine DBPs. For the hydrophobic fraction, the THMs and HANs concentration percentages show the different distributions, with the concentration percentage of the THMs components after chlorination being in the order of $\text{HiA} > \text{HoA} > \text{HiB} > \text{HoB} > \text{HiN} > \text{HoN}$. The concentration percentage of the HANs after chlorination was in the order of $\text{HoA} > \text{HoB} > \text{HiA} > \text{HoN} > \text{HiN} > \text{HiB}$. Compared to THMFP, the proportion of Br-HANs is higher, mainly because a certain amount of organic nitrogen compounds with unsaturated bonds exist in coking wastewater discharge. The formation of Br-DBP is related to characteristics such as molecular weight, hydrophobicity and chemical structure.

402 **3.5 3D EEM of molecular weight distribution**403
404

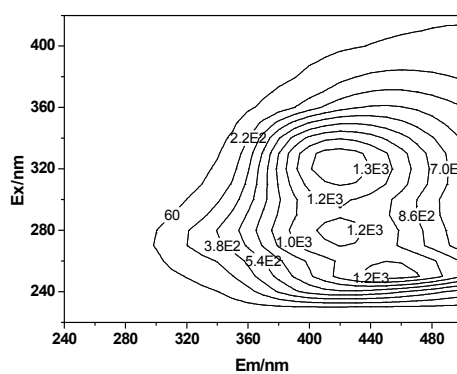
>100kDa



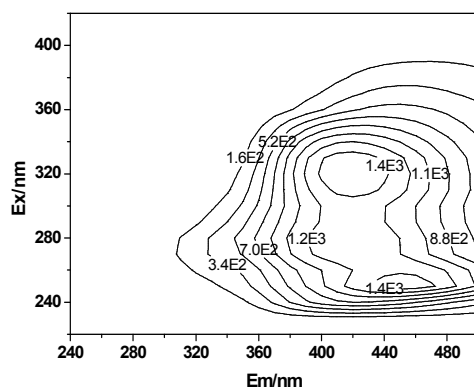
<100kDa

405
406

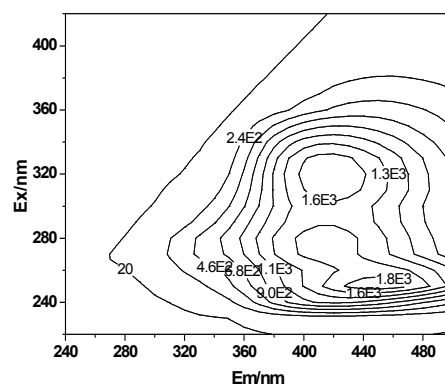
<30kDa



<10kDa

407
408

<5kDa



<1kDa

409 Fig. 7 3D EEMs of the molecular weight distribution in the control samples

410

411

412

413

414 Table 3 Analysis of 3DEEMs for molecular weight distribution

Molecular weight distribution	Peak A/ A'		Peak B/ B'		Peak C	
	E_x/E_m /nm	Fluorescence intensity/a.u.	E_x/E_m /nm	Fluorescence intensity /a.u.	E_x/E_m /nm	Fluorescence intensity /a.u.
>100 kDa	280/370	3415	330/380	1755	250/450	1688
< 100 kDa	280/420	1146	320/420	1369	250/450	1168
< 30 kDa	280/420	1178	320/420	1400	250/450	1196
< 10 kDa	280/420	1227	320/420	1455	250/450	1258
< 5 kDa	280/420	1411	320/420	1586	250/450	1549
< 1 kDa	280/420	1668	320/420	1748	250/450	1940

415 Previous studies demonstrated that treated wastewater effluent contained residual
416 DOM present in drinking water, soluble microbial products contributed during
417 biological sludge treatment and refractory DOM added by water users. In order to
418 trace the source of DOM and investigate the chemicals contributing to DBPs,
419 excitation emission matrices (EEM) were used to characterize different DOM
420 fractions^[20]. The contour maps of the results showed that different molecular weight
421 fractions exhibited different peaks (Figure 7). The fluorescence intensity
422 corresponding to the peaks are shown in Table 3. The DOM of treated coking
423 wastewater (>100 kDa) has three peaks, namely $E_x/E_m=280/370$ of fluorescence
424 intensity 3415 a.u, $E_x/E_m=330/380$ of fluorescence intensity 1755 a.u and
425 $E_x/E_m=250/450$ of fluorescence intensity 1688 a.u. Humic/fulvic acid, aromatic
426 proteins and some other soluble microbial by-products, such as protein-like or
427 phenol-like organics were found in the DOM fractions. After intercepting the
428 molecular weight of 100 kDa using membrane ultrafiltration, the emission wavelength
429 of the peak 280/370 redshifted by 50 nm, and at the same time, the strength weakened
430 by 49%. The area of solution fluorescent microbial metabolites has no fluorescence
431 peak. Other molecular weights <100, <30, <10, <5, and <1 kDa have the same peaks.

432 The results thus show that the soluble metabolic product is an important part of
433 treated coking wastewater in the >100 kDa molecular weight fraction. The same
434 fluorescence structures or organisms are also found in other fraction, which leads to
435 the phenomenon of peak overlapping. The fluorescence substance in the <1kDa
436 fraction thus needs to further analysis.

437 3.6 Precursors of THMs and HANs in treated coking wastewater by GC-MS

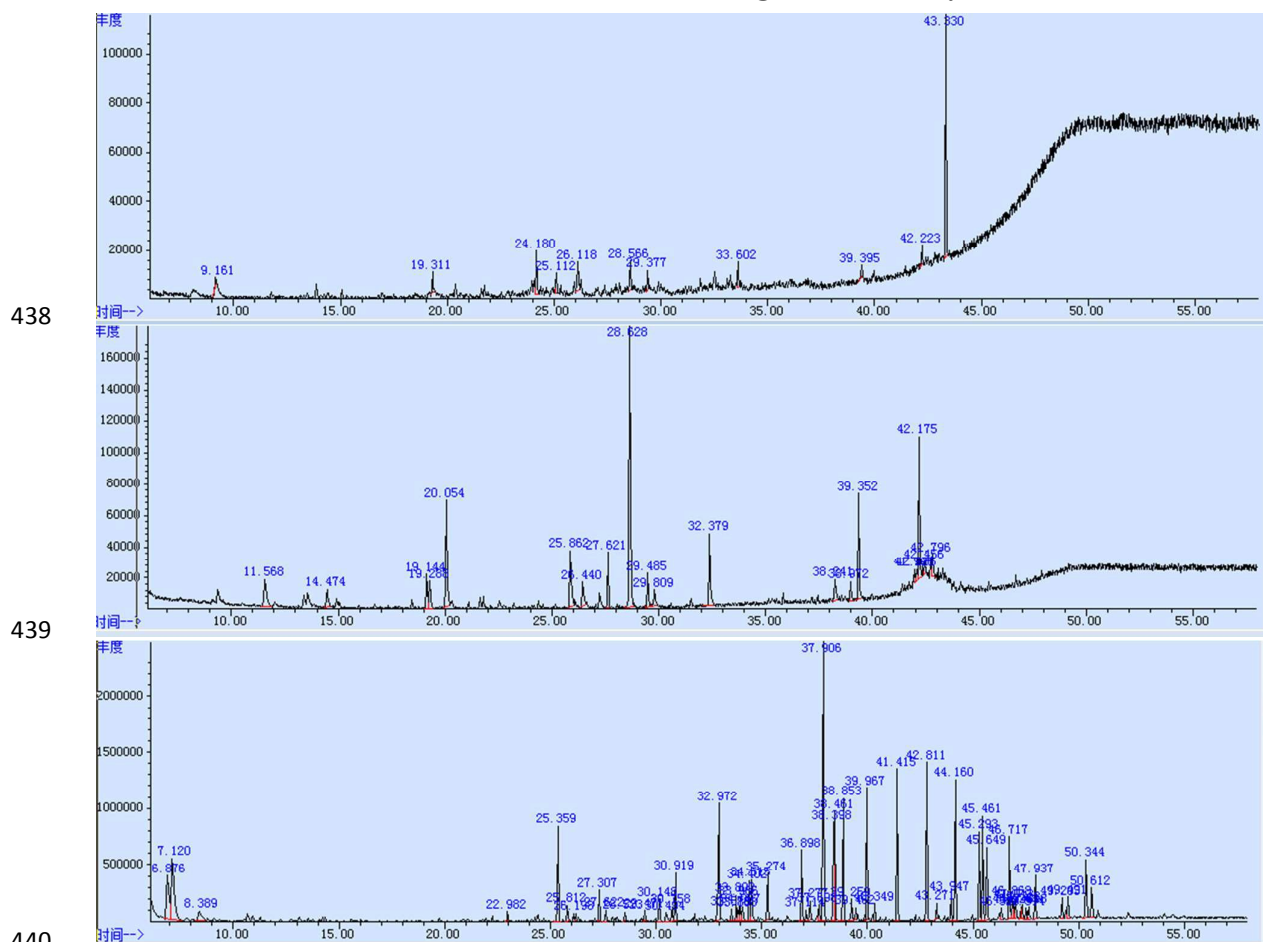
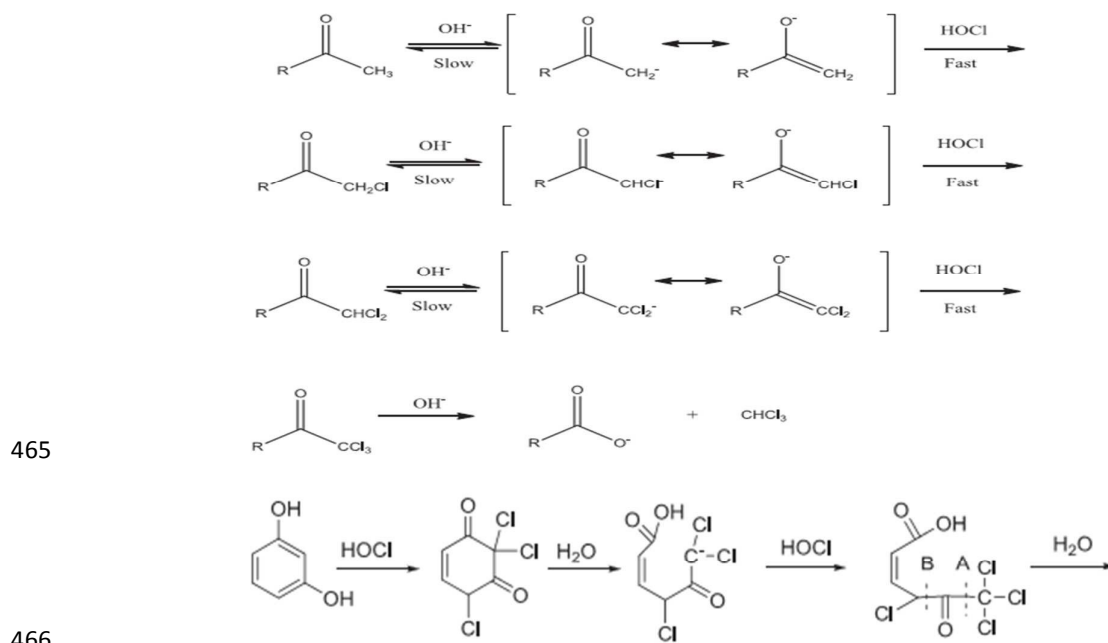


Fig. 8 GC-MS chromatogram of <1kDa molecule weight fraction by polarity (from top to bottom: non polarity, mid polarity and polarity)

Many studies have shown that DOC and DON serve as the main reactive precursors for DBP formation, and although much information has been obtained on this, such as the related structural characteristics, the detailed organic compounds of DOC and DON still need to be determined. Such knowledge would help in developing a more effective and economical approach to control these precursors when treating coking wastewater. Figure 8 shows the chromatogram of the <1kDa

449 molecule weight fraction. About 10 classes and 92 species were found in this fraction,
 450 including nitriles, amines, nitrogenous heterocyclic, hydrocarbons, polycyclic
 451 aromatic hydrocarbons, esters, phenols, alcohol, ketones, and organic acids, as shown
 452 in Table S1. In general, previous studies have identified a number of precursors which
 453 produce high levels of THMs and HANs^[33]. The most striking examples are
 454 carboxylic acids functional groups, amino acids, proteins, polypeptide, and
 455 carbohydrates. In contrast to coking wastewater discharge, nitrogenous heterocyclic
 456 and phenols would serve as new DBPs precursors. Schematics of the THMs and
 457 HANs formation pathways are shown in Figure 9^[28, 34-36]. It can be seen that the
 458 chlorine substitution reaction, chloride addition reaction, decarboxylic reaction, and
 459 dehydration reaction are the most important steps. In each fraction, both hydrophobic
 460 and hydrophobic organics have high chlorine reactivity with regard to the functional
 461 groups, such as carboxylate salt COO⁻, aromatic structures C=C, aldehydes and
 462 ketones groups C=O, carbohydrates C-C or O-alkyl group C-O. It is thus necessary to
 463 develop an appropriate technology if coking wastewater discharge is to be reused or
 464 released to surface water.



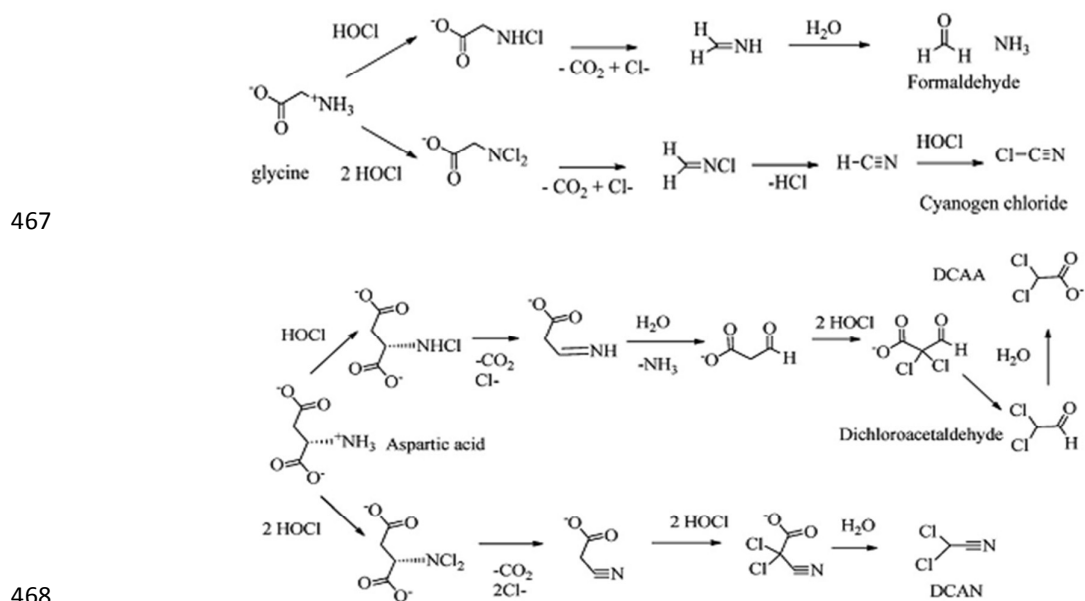


Fig.9 Schematics of the THMs and HANs formation pathways

4. Conclusions

471 DOM in the effluent from a coking wastewater treatment plant was fractionated
 472 using molecular weight and then divided based on resin adsorption into 42 classes.
 473 The DOM-fraction distribution, SUVA, source, molecular weight and chemical
 474 structure of the precursors were found to influence the formation of DBPs to a
 475 significant extent. Some new precursors were identified in coking wastewater
 476 discharge. The highest SUVA was found in the >100kDa fraction, at $12.1 \text{ L} \cdot \text{mg}^{-1} \cdot \text{cm}^{-1}$.
 477 The lower MW fractions (5-10k, 3-5k, 1-3k and <1kDa) had similar characteristics of
 478 SUVA, at about $4.1 \text{ L} \cdot \text{mg}^{-1} \cdot \text{cm}^{-1}$. The HiA fraction was found to be the most
 479 abundant, constituting about 45% of DOC. The THMFP and HANFP results showed
 480 that the DOM fraction with low MW and HiA was the dominant fraction and
 481 contributed more precursors. The EEM spectra indicated there were significant
 482 amounts of soluble microbial products and aromatic proteins in the >100 kDa fraction.
 483 The results of GC/MS analysis showed that nitriles, amines, nitrogenous heterocyclic,
 484 hydrocarbons, polycyclic aromatic hydrocarbons, esters, phenols, alcohol, ketones,
 485 and organic acids were the precursors in the <1 kDa fraction. All of these have high
 486 chlorine reactivity with regard to the functional groups, such as carboxylate salt COO^- ,
 487 aromatic structures $\text{C}=\text{C}$, aldehydes and ketones groups $\text{C}=\text{O}$, carbohydrates $\text{C}-\text{C}$ or

488 O-alkyl group C-O, which all contribute significantly to the formation of DBPs.

489

490 **Acknowledgment**

491 This research was supported by the Fundamental Research Funds for the Central
492 Universities (2013ZP0009) and the Key Program of National Natural Science
493 Foundation of China (21037001); Research Project of Production, Education and
494 Research of Guangdong Province, China (2012B091100450)

495

496 **References:**

- 497 [1] Jefferson G H. China's iron and steel industry: Sources of enterprise efficiency and the impact of
498 reform[J]. *Journal of Development Economics*, 1990,33(2):329-355.
- 499 [2] Worrell E, Price L, Martin Net al. Energy intensity in the iron and steel industry: a comparison of
500 physical and economic indicators[J]. *Energy Policy*, 1997,25(7):727-744.
- 501 [3] Zhang W, Wei C, Chai Xet al. The behaviors and fate of polycyclic aromatic hydrocarbons
502 (PAHs) in a coking wastewater treatment plant[J]. *Chemosphere*, 2012,88(2):174-182.
- 503 [4] Chenglong Y, Zhongjian S, Jinzhi Z. Problems and Solutions of Wastewater Treatment of Coking
504 Plant [J][J]. *Water & Wastewater Engineering*, 2000,6:10.
- 505 [5] Price L. A Comparison of Iron and Steel Production Energy Intensity in China and the US[J].
506 ACEEE Industrial Summer Study, New York, USA, July 2011, 2014.
- 507 [6] Lin C, Zhang W, Yuan Met al. Degradation of polycyclic aromatic hydrocarbons in a coking
508 wastewater treatment plant residual by an O3/ultraviolet fluidized bed reactor[J]. *Environmental
509 Science and Pollution Research*, 2014:1-10.
- 510 [7] Bond T, Goslan E H, Parsons S Aet al. A critical review of trihalomethane and haloacetic acid
511 formation from natural organic matter surrogates[J]. *Environmental Technology Reviews*,
512 2012,1(1):93-113.
- 513 [8] Bougeard C M, Goslan E H, Jefferson Bet al. Comparison of the disinfection by-product
514 formation potential of treated waters exposed to chlorine and monochloramine[J]. *Water research*,
515 2010,44(3):729-740.
- 516 [9] Chen B, Nam S, Westerhoff P Ket al. Fate of effluent organic matter and DBP precursors in an
517 effluent-dominated river: A case study of wastewater impact on downstream water quality[J].
518 *Water research*, 2009,43(6):1755-1765.
- 519 [10] Bond T, Huang J, Templeton M Ret al. Occurrence and control of nitrogenous disinfection
520 by-products in drinking water - a review[J]. *Water research*, 2011,45(15):4341-4354.
- 521 [11] Liang L, Singer P C. Factors influencing the formation and relative distribution of haloacetic
522 acids and trihalomethanes in drinking water[J]. *Environmental science & technology*,
523 2003,37(13):2920-2928.
- 524 [12] Krasner S W, Westerhoff P, Chen Bet al. Impact of wastewater treatment processes on organic
525 carbon, organic nitrogen, and DBP precursors in effluent organic matter[J]. *Environmental
526 science & technology*, 2009,43(8):2911-2918.
- 527 [13] Boyer T H, Singer P C. Bench-scale testing of a magnetic ion exchange resin for removal of

- 528 disinfection by-product precursors[J]. *Water Research*, 2005,39(7):1265-1276.
- 529 [14] Chen C, Zhang X, Zhu Let al. Disinfection by-products and their precursors in a water treatment
530 plant in North China: Seasonal changes and fraction analysis[J]. *Science of the total environment*,
531 2008,397(1):140-147.
- 532 [15] Navalon S, Alvaro M, Garcia H. Carbohydrates as trihalomethanes precursors. Influence of pH
533 and the presence of Cl⁻ and Br⁻ on trihalomethane formation potential[J]. *Water research*,
534 2008,42(14):3990-4000.
- 535 [16] Hua G, Reckhow D A. Characterization of disinfection byproduct precursors based on
536 hydrophobicity and molecular size[J]. *Environmental science & technology*,
537 2007,41(9):3309-3315.
- 538 [17] Marhaba T F, Mangmeechai A, Chaiwatpongsakorn Cet al. Trihalomethanes formation potential
539 of shrimp farm effluents[J]. *Journal of hazardous materials*, 2006,136(2):151-163.
- 540 [18] Zhao Z, Gu J, Fan Xet al. Molecular size distribution of dissolved organic matter in water of the
541 Pearl River and trihalomethane formation characteristics with chlorine and chlorine dioxide
542 treatments[J]. *Journal of hazardous materials*, 2006,134(1):60-66.
- 543 [19] Ates N, Kitis M, Yetis U. Formation of chlorination by-products in waters with low SUVA—
544 correlations with SUVA and differential UV spectroscopy[J]. *Water research*,
545 2007,41(18):4139-4148.
- 546 [20] Hao R, Ren H, Li Jet al. Use of three-dimensional excitation and emission matrix fluorescence
547 spectroscopy for predicting the disinfection by-product formation potential of reclaimed water[J].
548 *Water research*, 2012,46(17):5765-5776.
- 549 [21] Kim H, Yu M. Characterization of natural organic matter in conventional water treatment
550 processes for selection of treatment processes focused on DBPs control[J]. *Water research*,
551 2005,39(19):4779-4789.
- 552 [22] Zhang H, Qu J, Liu Het al. Characterization of isolated fractions of dissolved organic matter from
553 sewage treatment plant and the related disinfection by-products formation potential[J]. *Journal of*
554 *hazardous materials*, 2009,164(2):1433-1438.
- 555 [23] Huang H, Wu Q, Hu Het al. Dichloroacetonitrile and dichloroacetamide can form independently
556 during chlorination and chloramination of drinking waters, model organic matters, and wastewater
557 effluents[J]. *Environmental science & technology*, 2012,46(19):10624-10631.
- 558 [24] Díaz F J, Chow A T, O Geen A Tet al. Restored wetlands as a source of disinfection byproduct
559 precursors[J]. *Environmental science & technology*, 2008,42(16):5992-5997.
- 560 [25] The US Environmental Protection Agency method 551.1.
- 561 [26] Ou H, Wei C, Mo C al. Novel insights into anoxic/aerobic1/aerobic2 biological fluidized-bed
562 system for coke wastewater treatment by fluorescence excitation–emission matrix spectra coupled
563 with parallel factor analysis. *Chemosphere*, 2014, 113, 158-164.
- 564 [27] The national discharged standards of China. GB 12356-2012.
- 565 [28] Boyce S D, Hornig J F. Reaction pathways of trihalomethane formation from the halogenation of
566 dihydroxyaromatic model compounds for humic acid[J]. *Environmental science & technology*,
567 1983,17(4):202-211.
- 568 [29] Sirivedhin T, Gray K A. 2. Comparison of the disinfection by-product formation potentials
569 between a wastewater effluent and surface waters[J]. *Water research*, 2005,39(6):1025-1036.
- 570 [30] Liu J, Li X. Biodegradation and biotransformation of wastewater organics as precursors of
571 disinfection byproducts in water[J]. *Chemosphere*, 2010,81(9):1075-1083.

- 572 [31] Chang H, Chen C, Wang G. Identification of potential nitrogenous organic precursors for C-,
573 N-DBPs and characterization of their DBPs formation[J]. Water research,
574 2011,45(12):3753-3764.
- 575 [32] Sun Y, Wu Q, Hu Het al. Effect of bromide on the formation of disinfection by-products during
576 wastewater chlorination[J]. Water research, 2009,43(9):2391-2398.
- 577 [33] Chu W H, Gao N Y, Yin D Qet al. A predictive model for the formation potential of
578 dichloroacetamide, a nitrogenous disinfection by-product formed during chlorination[EB/OL]. [4].
579 <http://link.springer.com/10.1007/s13762-012-0104-0>
580 <http://www.springerlink.com/index/pdf/10.1007/s13762-012-0104-0>.
- 581 [34] Bond T, Templeton M R, Graham N. Precursors of nitrogenous disinfection by-products in
582 drinking water - - a critical review and analysis[J]. Journal of hazardous materials,
583 2012,235:1-16.
- 584 [35] Deborde M, von Gunten U. Reactions of chlorine with inorganic and organic compounds during
585 water treatment — kinetics and mechanisms: a critical review[J]. Water research,
586 2008,42(1):13-51.
- 587 [36] Joo S H, Mitch W A. Nitrile, aldehyde, and halonitroalkane formation during
588 chlorination/chloramination of primary amines[J]. Environmental science & technology,
589 2007,41(4):1288-1296.
- 590